LA-UR -92-46

Los Alamos National Laboratory is operated by the University of California for the United States Department of Energy under contract W-7405 -ENG-36.

TITLE: TARGET/BLANKET CONCEPTUAL DESIGN FOR THE LOS ALAMOS ATW CONCEPT

AUTHOR(S): John R. Ireland and Michael W. Cappiello, N-12

SUBMITTED TO: Specialists' Meeting on Accelerator-Based Transmutation
Paul Scherrer Institute (PSI)
Wuerenlingen/Villigen, Switzerland
March 24-26, 1992

Los Alamos Los Alamos National Laboratory
Los Alamos, New Mexico 87545

FORM NO 836 R4
ST No 2629 5/81

TARGET/BLANKET CONCEPTUAL DESIGN FOR THE **LOS ALAMOS ATW** CONCEPT

January 1992

AUTHORS AND ACKNOWLEDGMENTS

AUTHORS:	M. Cappiello
	J. Ireland
	J. Sapir
	G. Farnum
CONTRIBUTORS:	G. Russel
	W. Sommer
	W. Rider
	B. Krohn
	W. Wilson
	R. Perry
	R. LaBauve
	P. Lisowski
	E. Arthur
	L. Linford
	C. Cummings
	C. Cappiello
	R. Manzanares
EDITORIAL:	K. Ames
WORD PROCESSING:	G. Mirabal

TARGET/BLANKET CONCEPTUAL DESIGN FOR THE LOS ALAMOS ATW CONCEPT

I. INTRODUCTION

The Los Alamos Accelerator Transmutation of Waste (ATW) concept has many potential applications that include defense waste transmutation, defense material production (i.e., tritium and ^{238}Pu), and the transmutation of hazardous nuclear wastes from commercial nuclear reactors (fission products and actinides). A more advanced long-term Los Alamos effort is investigating the potential of an accelerator-driven system to produce fission energy with a minimal nuclear waste stream. All applications employ a high-energy (800- to 1600-MeV), high-current (25-250 mA) proton linear accelerator as the driver. In this report, we discuss only the target/blanket conceptual design for the commercial nuclear waste application.

The basis of all ATW applications is the use of high-energy protons from a linear accelerator to produce neutrons through spallation instead of nuclear chain reactions. The protons are directed onto a high-atomic-number target material to produce neutrons, which are then moderated in a surrounding heavy-water (D_2O) blanket. The neutrons are slowed to thermal energy in the moderator and are absorbed in the fission product waste, or they are used in the fission and transmutation of actinides. Because of the intense flux of generated neutrons, fission products that have small neutron absorption cross sections, such as ^{99}Tc, can be transmuted to stable isotopes in significant quantities. Fissile actinides such as ^{239}Pu can be fissioned directly.

Because of the high flux levels, very dilute mixtures in the blanket region can be used, which therefore reduce the potential for criticality accidents and power excursions. The transmutation isotopes are continuously transported in double-walled piping systems through the blanket region, through heat exchangers, and into separation process loops. Heavy-water aqueous solutions and slurries are used as the transport media.

II. DESIGN SUMMARY

A schematic of the base-case ATW design is shown in Fig. 1. The linear accelerator operates at 1600 MeV at a continuous-wave current of 250 mA. The primary proton beam is then split into four beams, each having a current of 62.5 mA and an energy of 1600 MeV. Each of the four beams is directed into four separate target/blanket modules. A modular design approach allows maintenance or replacement of components with relative ease and adds to the overall

reliability of the system. The modules have separate cooling loops for their respective targets, moderators, and blankets, and operate independently from each other.

The high-energy proton beam strikes a centrally located spallation target to produce an intense source of neutrons. The base-case target design is comprised of heavy-water-cooled tungsten rods. The power density is very high, and therefore requires sub-cooled boiling as the heat-transfer mechanism. Because of the intense proton and neutron environment, the target assembly will require routine replacement

Each target/blanket module is designed to burn the actinides and fission products from approximately two light-water reactors and produce approximately 1542-MW_t power. Figure 2 shows a schematic of the blanket and balance-of-plant components for electric energy production. The blanket region and balance-of-plant design is based on existing heavy-water reactor technology employed in the CANDU reactor system. Here, the fuel is contained in double-walled pressure tubes that pass through the blanket-

One main difference between the CANDU design and the ATW design is that an aqueous homogeneous continuous flow primary loop is employed in the ATW design, whereas solid heterogeneous fuel is used in CANDU. It is necessary to use the liquid fuel approach for actinide burning in ATW to take advantage of the high neutron flux and the rapid burn rates, as well as facilitate the continuous processing. This approach complicates the design somewhat because the fuel will be circulated both inside and outside the blanket region. To prevent the radioactive liquid fuel from coming into contact with the steam loop that drives the turbine-generator set, an intermediate light-water heat-transfer loop is added The additional intermediate loop adds another degree of safety margin in case of accidental radioactive release from a rupture from the liquid fuel primary loop. The heat from the intermediate loop is transferred to a light-water secondary loop for steam generation. In this concept, energy produced in the blanket from the fission of the actinides is recovered and used to produce electricity with about 30% thermal efficiency. This recovery of useful energy greatly reduces the overall cost of the facility.

A proposed layout for the target/blanket is shown in Fig. 3. The solid tungsten/lead target is surrounded by an annulus of technetium in D_2O, an actinide slurry region, and a D_2O reflector. The target/blanket design is evolving in an effort to enhance the safety, reliability, and efficiency (with respect to neutron utilization). For example, it may be possible to keep the actinide slurry within the blanket region, and transfer heat to the heavy-water moderator that is pumped outside the blanket. This retention will greatly reduce the overall volume of actinide slurry and reduce the risk of spills outside the blanket.

Another option that is being considered is the use of a flowing liquid lead target. The use of such a target adds complexity to the design but has the potential to increase the neutron utilization efficiency. In addition, if greater accelerator currents are required, the liquid target can

more easily remove the heat. The base-case target/blanket design and some of the design options are presented in more detail below.

111. TARGET/BLANKET DESIGN OBJECTIVES

The design of the target/blanket region for ATW is complex. As the target intercepts the proton beam, the heating rates are exceptionally high (9 MW/l peak) and the neutron flux levels produced are much higher than those for commercial nuclear reactors. The neutrons are very expensive to produce when an accelerated proton beam is used. Therefore, the design of the target/blanket is crucial; it must use the neutrons as efficiently as possible while maximizing safety and reliability considerations. We have specified several goals in the design of the target/blanket (values given are for one light-water reactor waste discharge):

- transmute 33 kg of technetium and 7 kg of iodine per year;
- transmute 300 kg of actinide mixture per year (neptunium, americium, plutonium);
- minimize parasitic capture in structures and target;
- use materials that are compatible with fluids to minimize corrosion;
- use materials that avoid generation of long-lived radioactive nuclides;
- use materials that can withstand intense irradiation,
- provide a safe system that will easily meet nuclear facility licensing and safety goals;
- maintain subcriticality during normal and off-normal situations;
- use passive modes of heat removal where possible;
- ensure easy operation and maintenance; and
- minimize long-tam research and development activities and costs.

IV. TARGET DESIGN OPTIONS

The protons from the split beam are directed onto the neutron production target region. There are several high atomic number materials that can be used for the spallation target including lead (Pb), lead-bismuth (Pb-Bi), tungsten (W), tantalum (Ta), and uranium (U). Through spallation in a lead target, approximately 50 neutrons are produced for each incident 1600-MeV proton. Neutron production is reduced to about 22 neutrons per proton for the 800-MeV application, and if a tungsten target is used, the neutron production decreases to approximately 18 neutrons per proton for the 800-MeV accelerator. For heat transfer and power density considerations, approximately 75% of the thermal energy in the beam is deposited directly into the

target; the remainder of the power is removed by neutrons and gammas that leak into the blanket. For the 1600-MeV, 62.5-mA proton beam, approximately 100-MW_t power is generated, of which 75 MW_t is deposited in the target.

For the ATW commercial waste application, two target design options have been considered. The base-case design uses solid tungsten rods cooled with heavy water. As an option, a flowing liquid lead or lead-bismuth system is proposed, either of which act as the spallation target material and heat transport medium.

A. Solid Target Design

The solid target is made of separate regions of tungsten and lead (Fig. 4). Because of its high melting point (3300" C), tungsten would be used primarily in the high thermal energy region of the target. Because the interior of the solid target is pressurized, a window is required to separate the accelerator vacuum from the target region. For this configuration, heavy-water cooling is required for the window and the tungsten rods to keep the temperature gradients at reasonable values. The neutron absorption in D_2O is small and has the added benefit of moderating the neutrons. However, D_2O will interact with the proton beam and cause some degradation in neutron production.

A region of solid lead surrounds the tungsten target. The lead provides a boost in the neutron production from additional spallation and (n,xn) reactions. The lead is cooled with D_2O to keep it well below the melting point. A disadvantage to using tungsten as the main target material is that it has a significant neutron absorption cross section. Enriching the tungsten in the isotope ^{184}W would reduce the absorption approximately by a factor of 10 but would be very expensive. To increase the neutron leakage from the tungsten and therefore reduce the parasitic absorption, we have introduced flux traps in the spaces between the tungsten rod units. We have successfully demonstrated this concept at the Los Alamos Neutron Scattering Center (LANSCE).

1. **Target Detail.** The target is designed as a separate assembly that can easily be removed and replaced during routine maintenance. The target assembly consists of a spherical shaped window, several tungsten rod units, and coolant pipes. The entire assembly is encased in a single structure and is removed and replaced as a single component. The window and tungsten rod units are cooled with D_2O. The regions between the tungsten rod units are filled with helium gas that is at a slightly higher pressure than the D_2O coolant (about 3.4 M_Pa), which maintains a compressive force on the container of each unit and reduces the mechanical stress. The window and the containers for the individual tungsten units are made of Inconel 718. The structural container for the entire assembly is made of an aluminum alloy.

2. **Window**. At high-energy accelerator facilities, a metal interface is used to maintain a vacuum in the accelerator and to protect the equipment in the experimental area. Because of the

intense energy of the ATW accelerator, a windowless system is desirable, and it is possible that the flowing liquid target may provide that capability. However, if a solid target is used, a window is required. Even if the liquid target is used, it may be necessary to first test the system with a window to determine if the vacuum pumps can keep up with the pressure demand before actual operation takes place without a window. Therefore it is important to study existing window designs and to determine their applicability to ATW.

Results of research at the Los Alamos Meson Physics Facility (LAMPF) have provided considerable data about window survivability. The LAMPF accelerator is 800 MeV, 1 mA. The double-walled flat window used on the current beam stop at LAMPF has undergone 17,500 h at 20-30 $\mu A/cm^2$, for a total proton fluence of 1.3e22 p/cm^2. This window is made of Inconel 718. Another Inconel window is used for the vacuum-t-air interface. It is replaced yearly and accumulates approximately 2.9e21 p/cm^2. The proposed window for the Swiss Nuclear Institute Neutron Source (SINQ) is being tested at LAMPF. This material is a steel (Fe10.5Cr) and has also accumulated 2.9e21 p/cm^2 of fluence proton.

For comparison to AlTV, we assume that the 1600-MeV, 62.5-mA proton beam is roughly equivalent to 800 MeV, 140 mA with respect to material damage. This provides an average flux of about 224 $\mu A/cm^2$ and in one full-power year 3.52e22 p/cm^2 of proton fluence. This fluence is a factor of 2.7 times the current fluence on the LAMPF beam stop still in service. Based on this experience, it may be reasonable to assume that a window in ATW would require replacement about every 6 months.

3. Tungsten Rod Units. The proton beam that strikes the target is a 25-cm square spatial pattern with a nearly flat intensity profile. The tungsten rod units are also square and are 30 cm on a side. The D_2O coolant enters one side of the unit through an inlet plenum and exits the opposite side through a similar plenum. The coolant feed for each unit is separate, which allows for pressure and integrity checks before final assembly. Because the beam degrades as it passes through the units, there is a reduction in the power density from one unit to the next. To flatten the axial power distribution and the neutron source, we vary the amount of tungsten in each unit. An orifice between each unit may be required. In the horizontal direction, because the power density is flat across the tungsten square, there is no need for orifices within each individual unit. Although the rod units are square, they fit inside a cylindrical structure that is about 40 cm in diameter. The rest of the surrounding blanket is also cylindrical.

Within a single tungsten rod unit, the rods are encased in a thin shell of Inconel 718 (Fig. 5). This contains the D_2O coolant and provides a structural support for the rods. The rods are set in several sets of two rows, each with flow passages in between. From a distance, the rods appear to form a plate with a bumpy surface. The rods are held in place at the ends in a manner that allows them to expand and contract, which thereby significantly reduces the thermal and

mechanical stresses. The number of rod sets (or "plates") in each unit can vary to flatten the axial power distribution. In each unit, the tungsten occupies about 50% of the free volume. The rest is occupied by the D_2O coolant.

4. Heat-Transfer Analysis. Detailed heat-transfer calculations were performed for a typical channel in the peak power density region (the tungsten unit that is first hit by the proton beam). In this region, the calculated power density in the tungsten is 8.64 MW/l, and in the D_2O 0.327 MW/l. For our geometry, this is equivalent to a heat flux of about 10.8 MW/m^2. For the heat-transfer analysis, "plate" geometry was assumed with the plate thickness equivalent to a two-row set of rods. The calculations were performed with a multiphase flow code that can predict the onset of boiling with reasonable accuracy. The tungsten "plate" was modeled as a slab with 30 axial nodes placed along its length. Each axial node *contained* 10 horizontal nodes to resolve the temperature distribution between the middle of the "plate" and the surface that is in contact with the coolant. The results show that for a coolant pressure of 5 MPa, inlet temperature 300 K, and a velocity of 13 m/s, the flow will remain single phase. The peak tungsten temperature is about 450 K, which is small compared with the melting point (3800 K). If subcooled boiling is used as the heat-transfer mechanism, the pressure may be reduced significantly. Experimental results for fusion reactor applications (Refs. 1–3) show that heat fluxes greater than 20 MW/m^2 may be obtained. Therefore, it appears that adequate cooling can be achieved.

The hydraulic design of the target will be verified with full-scale tests to experimentally check the flow distribution through the assembly and each tungsten unit. Subscale tests will be used to verify the thermal design to ensure that cooling is adequate for both normal and off-normal conditions.

5. Decay Heat. The decay heat has been predicted for the main components of the target assembly using the LAHET/MCNP/CINDER code system. The results show that after 1 year of operation at 80% availability, the decay heat in the tungsten amounts to 0.4% of the total heat generated at full power. *This* heat decays quickly and after 1 day is down to 0.1 %.

B. Liquid Target Design

The flowing liquid spallation target is a pure lead material (melting point 600 K). The lead target material has a high atomic number, good heat-transport properties, and is compatible with low-chronium, low-nickel stainless steel alloys such as Croloy. A lead-bismuth eutectic was originally chosen as the material of choice for the liquid target option because of its low melting point, high boiling point, low vapor pressure, and high atomic number. However, because of the production of ^{210}Po from the bismuth (a major radiologic hazard), this material has fallen out of favor. Instead, lead is now the material of choice and is the focus of much of our attention for the flowing target system. Although lead operates at a higher temperature, it appears the difficulties

with respect to cooling, vapor pressure, and operation can be overcome. Evidently, the Soviets have experience with liquid lead coolants for some of their reactors. Still, lead produces some long-lived waste products when irradiated in the proton beam and becomes a mixed waste (toxic and radioactive). When compared with the solid tungsten target, this puts the flowing lead system at a disadvantage. One advantage of the flowing liquid lead design is that a window between the beam and the target may be unnecessary if the vapor pressure of the liquid at the surface is sufficiently low that the vacuum may be maintained.

The orientation of the flowing liquid target is vertical with the liquid lead flowing upward through an annulus, turning, and then flowing downward into a cone-shaped open channel. Here the fluid interacts with the proton beam and is in direct contact with a vacuum. As the target material is flowing downward through the channel, the spallation reactions cause significant heat generation. The fluid coalesces in the central target area that is about 50 cm in diameter and flows downward at about 2 m/s. The flow rate is sufficiently high to convect the heat away at a reasonable temperature. In the target region, the bulk temperature increase is 100 K (from 700 K to 800 K). The flow exits the bottom of the target region and is pumped through a heat exchanger. The heat is transferred to a secondary sodium-potassium (NaK) eutectic heat-transport loop and then dumped to the atmosphere through a forced-air heat exchanger. The loop components such as the pump and heat exchanger will require development and testing to ensure an adequate design. The NaK system and dump heat exchanger are similar to the heat dump system used in the Fast Flux Test Facility.

The neutron damage to the container wall may require replacement every 1 or 2 years. The intense flux occurs in a relatively small 50-cm section of the wall. Here the static head of fluid is very low (0.09 MPa or 13.2 psi) and the calculated hoop stress only 4.68 MPa (680 psi). Because of the low stress, material lifetimes may be increased. A double-wall construction is required to provide thermal insulation between the target and the blanket, and to prevent liquid metal-water interaction in the event of a leak.

V. BLANKET DESIGN

The ATW blanket design for each of the four modules is based on the existing CANDU reactor design. The primary reasons for this choice is that the CANDU system uses heavy water as the coolant and moderator, and the power level is approximately the same for each module as in the CANDU-3. Therefore, ATW can benefit from this experience base, which will minimize overall research and development costs.

A. Comparison to CANDU Heat Transport System

Table 1 provides a comparison of key design parameters for CANDU-3 and one target/blanket module of ATW.

B. MATERIAL COMPATIBILITY

The current ATW base-case design employs zirconium alloys for containment vessels and piping in heavy-water-cooled environments. Temperatures from < 100° Cup to 300° C are anticipated. Neutron flux of about 2 E 15 n/cm^2-s is anticipated and the neutron spectrum varies between mostly thermal and mostly fast-reactor-like, but because of a lead shield, not spallation-like. In addition, the presence of technetium salts in the shiny require that the pH of the slurry be approximately 11. With respect to the performance of zircaloys in the anticipated environment there is a wealth of information.

Zircaloys were developed for cladding in light-water reactors. Therefore their performance in a thermal neutron spectrum and water environment is excellent. In the above application, zircaloys will perform adequately provided a number of precautions are addressed.

It is important to note that almost every light-water reactor in the world has been shutdown at least once because of corrosion problems, so no system is likely to be perfect. The zircaloys are the best materials at moderate temperatures (< 400° C) in water environments. Zircaloys (and all other reactor metals) are reactive with water and obtain their protection from a tightly adherent oxide surface layer. Light-water reactors typically add LiOH to the water to obtain a pH of 9 to 11 as a corrosion inhibiter. At a higher pH, LiOH enhances corrosion. The mechanism of LiOH inhibition is not completely understood, but lithium interaction with the oxide protective layer is thought to play a role. Therefore, it is likely that technetium salts with a pH of 11 will not be corrosive to zircaloys, but some caution is required.

In addition, corrosion in zircaloys is enhanced by dissolved oxygen in the water. Zircaloys are sensitive to hydrogen embrittlement. Hydrogen enters the alloy by the reaction $Zr + H_20 \rightarrow ZrH + O$. ZrH forms interstitial platelets that decrease the alloys' strength. At much higher temperatures such as would be experienced in a reactor coolant loss, zirconium reacts with water to form hydrogen gas by the reaction $Zr + H_20 \rightarrow ZrO_2 + 2H_2 + 140$ kcal/mole. This situation obviously causes an explosive hazard. Zircaloy-4 is similar to zircaloy-2 except that zircaloy-4 has no nickel content.

Zircaloys have been irradiated up to 100 displacements per atom (dpa) thermal neutron fluence. The amount of swelling and the decrease in ductility caused by thermal neutrons is known and can be accommodated by proper design. However, many variables are important in determining the response of any material to irradiation and extrapolation to different conditions is

not straightfonvard. Performance (expected service life) will be dependent on the irradiation temperature and flux, the neutron spectrum, and chemistry of corrosion.

Erosion is an issue with ATW systems using metal-oxide (ceramic particulate) slurries. Flowing water enhances corrosion, especially at bends in tubing and in pumps. Because the materials depend on an oxide layer to prevent corrosion, an abrasive slurry that abrades or pits the layer will increase the corrosion rate. This effect can be very severe at high flow velocities. Overall, for the current ATW application, zircaloy-4 would be the preferred alloy.

VI. PRELIMINARY PHYSICS ANALYSIS OF THE BLANKET

The aqueous blanket incorporates a flowing D_2O "slurry" of pressurized water reactor actinide wastes contained in CANDU-type pressure tubes. The double-walled pressure tubes are immersed in a D_2O moderator that surrounds the neutron-producing target. Long-1ived fission-product wastes are circulated through the blanket, either directly in the moderator or in separate tubes.

The composition of the actinide waste was obtained from an ORIGEN point depletion calculation using a CANDU neutron spectrum. Table 2 shows the relative isotopic composition of the light-water reactor actinide wastes and the equilibrium composition after irradiation in a flux of 1.0 x 10^{15} that was used in our calculations. Plutonium isotopes constitute almost 90% of the feed material mass but only 50% of the equilibrium mass. The primary fissile isotopes are ^{239}Pu and ^{241}Pu.

A. LATTICE CELL CALCULATIONS

Figure 6 shows a schematic of the lattice cell employed in our initial calculations. The cell contains the actinide slurry surrounded by double-walled zirconium pressure tubes and the associated D_2O moderator. Dimensions and area fractions are shown for the configuration that was eventually chosen for the reference design.

Initial calculations investigated the effects of actinide concentration, tube size, and tube spacing on k_{eff} (or k_∞ in the case of the non-leakage unit cell). Figure 7 shows the dependency of k_∞ on actinide concentration. Initially increasing the actinide concentration from 5 g/1 has a pronounced positive effect on k_∞, but the curve flattens out at approximately 30 g/1. At low actinide concentrations, the neutron balance is dominated by captures in the zirconium tubes, which account for 60% of all captures at 5 g/1. Initial introduction of fissile material effectively competes with the zirconium captures, reducing those captures to 13% at 50 g/1 where that effect becomes relatively small. However, increasing the actinide concentration also hardens the neutron spectrum in the slurry, which increases the epithermal and resonance captures in the non-fissile isotopes

(primarily ^{240}Pu and ^{242}Pu) relative to the predominantly thermal fission reactions in the fissile isotopes. Once the zirconium captures become less important, the spectral-hardening effect tends to mitigate further increases in k_∞. A finite system might continue to exhibit an increasing k_{eff} dependency if the addition of fissile material competes with neutron leakage. However, the proposed ATW blanket is a relatively large, low leakage system, and should show the same behavior as found in the lattice-cell calculations. Therefore, for the hexagonal lattice configuration used in these calculations (10-cm-diam. tubes spaced 17.0 cm apart), it appears that the maximum attainable k_∞ is approximately 1.0. Considering that we need additional reactivity to compensate for leakage, target, and structure absorption, as well as fission product poisoning and burning, it is doubtful that this value of k_∞ will provide the high multiplication needed for satisfactory system performance.

The effects of the slurry-tube radius and pitch are shown in Figs. 8a and 8b, which are parametric plots of the same data. For the tube-size investigation, the relative areas of slurry, walls, and moderator were maintained as the cell dimensions were varied. Figure 8 shows that at a given pitch, k_∞ increases only slightly with increasing tube size, but increasing the tube pitch (spacing) can yield significant improvements in k_∞. A larger tube pitch increases the moderator/slurry ratio. This allows fission neutrons that leave the slurry to slow down and thermalize in the D_2O moderator before returning to the slurry, thereby reducing the probability of resonance capture in the nonfissile actinides. This effect can be seen in Fig. 9, which plots the actinide capture-to-fission ratio as a function of tube spacing (capture is defined as a non-fission absorption). Increasing the pitch strongly reduces the overall parasitic capture probability. Because a constant actinide slurry area is required for heat-transport considerations, increasing the slurry/moderator ratio will also increase the blanket size.

The final cell calculations extended the range of actinide concentrations up to 100 g/l. These results are shown in Fig. 10. The lower curve in Fig. 10 is an extension of the plot in Fig. 7 and confirms the inability to increase k_∞ for that configuration (17.0-cm pitch). However, at the larger spacings, increasing the actinide concentration can achieve further gains in k_∞.

Based on these cell calculations, we selected a 5-cm-radius tube, a 23.8-cm pitch, and a 75-g/l actinide concentration as the reference lattice configuration to be used in the blanket calculations. The resulting value of k_∞, shown in Fig. 5 as a large dot, is 1.158. A neutron balance for the reference lattice-cell configuration is shown in Table 3.

B. BLANKET CALCULATIONS

A schematic of the target-blanket configuration is shown in Fig. 3. The target is a homogenized version of the solid tungsten rod design. Primary regions in our one-dimensional model are the homogenized tungsten rods, a Pb-D_2O region, an aluminum target structure, and a

zircaloy tank wall followed by a thin 1 molar Tc/D_2O buffer region whose thickness was varied. A D_2O outer reflector surrounds the "active" actinide blanket region.

Because ONEDANT is a one-dimensional code (cylindrical geometry in this case) that cannot accept azimuthal geometry changes, we must homogenize the lattice cell for incorporation into the blanket calculations. This was done by flux-volume-weighting the constituent materials and the cross sections in the unit cell to preserve reaction rates. The accuracy of this approximation must be checked by a more rigorous MCNP calculation that can more accurately model the detailed geometry.

Before homogenizing the lattice cell, we incorporated ^{10}B into the actinide slurry to simulate the buildup of fission products (excluding technetium and iodine). The ^{10}B concentration was adjusted to produce the same fission product absorption rate relative to the total actinide absorption that were calculated for a 10-day buildup at a flux of 1.0×10^{15}. The addition of the appropriate amount of ^{10}B reduced the k_∞ of the lattice cell by 0.057 Δk.

The blanket calculations incorporated the homogenized (flux-weighted) cell cross sections that contained the ^{10}B simulated lumped fission products. The k_{eff} of an infinite-length blanket configuration was 0.057 Δk less than the corresponding cell value. This reduction is due to radial leakage and neutron capture in blanket materials. An additional 0.035 was lost in the inclusion of an axial-leakage approximation into the one-dimensional calculation. The resulting blanket k_{eff} was 1.008.

The next step in the blanket calculations was to simulate burning of long-lived fission products produced in the pressurized water reactor cycle as well as in the blanket itself. Again, relative neutron captures per fission required to bum technetium and iodine were obtained from the ORIGEN calculation. The following procedure was followed for these calculations:

1. An operating value of k_{eff} was selected
2. To simulate fission product burning, an eigenvalue calculation was performed in which technetium was added homogeneously throughout the actinide region and the outer reflector to reduce the k_{eff} from the initial value of 1.008 to the target value selected in step 1.
3. A source problem was run with the appropriate technetium concentration determined in step 2.
4. Results from step 3 (power and the ratio of technetium captures per fission) were normalized to a 800-MeV, 140-mA beam (or equivalently to a 1600-MeV, 62.5-mA beam) and compared with the goal values required to support two light-water reactors.

5. The above steps were repeated for varying thicknesses of the inner Tc/D_2O buffer region.

These steps were followed for operating k_{eff} values of 0.95 and 0.93. The results are shown in Figs. 11 and 12, respectively. Two figures of merit are plotted as a function of the $Tc-D_2O$ buffer region thickness: (1) the blanket power and (2) the technetium bum rate, both relative to the respective goal values required to service two pressurized water reactors. From Fig. 7 we see that at an operating k_{eff} of 0.95 and no technetium buffer region, sufficient neutron multiplication exists to produce approximately 1.2 times the 1640 MW needed to burn the actinide wastes from two pressurized water reactors. However, at this relatively high k_{eff} there are not enough excess neutrons available to burn the required technetium atoms (only 72% of the goal technetium burn is achieved). Increasing the buffer region thickness puts technetium atoms in a high flux region and increases the technetium captures relative to the fissions. However, capturing the source neutrons before they are multiplied in the actinide region reduces the effective multiplication and the resulting power. These conflicting trends are shown in Figs. 11 and 12. At the point where the two curves intersect, the two parameters (actinide and fission-product burn) are balanced for the needs of the pressurized water reactor cycle. At a k_{eff} of 0.95 and a buffer region thickness of 1.9 cm, the blanket will operate at a power level of 1542 MW and support 1.88 pressurized water reactors. A neutron balance for this configuration is shown in Table 4.

Operating at a k_{eff} of 0.93 allows the incorporation of more technetium atoms and provides more excess neutrons so that for a given buffer-region thickness more technetium will be burned. However, Fig. 12 shows that even with no buffer region, the blanket will burn only 88% of the technetium goal amount. At a k_{eff} of 0.93 there is also insufficient multiplication to meet the power goal, and adding a buffer region to increase the technetium burn will further aggravate the power deficiency. Thus, a blanket operating at a k_{eff} of 0.93 would not have any technetium buffer region and would service the equivalent of approximately 1.7 pressurized water reactors.

In calculating the achievable technetium bum, we included radial neutron leakage as being captured in technetium. This could be achieved by increasing the technetium concentration in the outer part of the radial reflector and/or by making it thicker.

The reference blanket has an actinide inventory of 325 kg in a 250 cm length. The corresponding technetium inventories are 82.0 and 99.2 kg in blankets operating at a k_{eff} of 0.95 and 0.93, respectively. The one-dimensional fluxes in the actinide blanket were calculated to be 1.38×10^{15} and 1.26×10^{15} $n/cm^3\text{-}s$ for k_{eff}s of 0.95 and 0.93, respectively. The two-dimensional fluxes will probably be lower throughout a significant part of the blanket.

In summary, we have performed one-dimensional physics calculations to investigate the performance of an aqueous ATW blanket to burn actinides and long-lived fission products from the

pressurized water reactor fuel cycle. These calculations indicate that a blanket combined with a 800-MeV, 140-mA (or equivalently a 1600-MeV, 62.5-mA) accelerator maybe able to transmute wastes from almost two pressurized water reactors.

These calculations must be considered very preliminary. They are based on equilibrium actinide and fission product concentrations calculated from a point depletion code using a CANDU neutron spectrum. Because the blanket performance is very sensitive to data derived from these depletion calculations, a second iteration using flux and spectra determined from the initial blanket study must be performed. Also, more rigorous two- and three-dimensional physics calculations must be performed to check the accuracy of the one-dimensional calculations and to account for spatial effects. Eventually, two-dimensional depletion calculations should be performed on the blanket design, not just for equilibrium operation, but for the entire ATW operating cycle. Additional cross-section generation effort is also needed. In particular, we need cross sections for several actinides not currently available, such as ^{248}Cm, and for D_2O at the relatively high slurry temperature of 600 K.

VII. CONCLUSION

A conceptual design for the target/blanket of the Los Alamos ATW concept has been presented. The neutronics, mechanical design, and heat transfer have been investigated in some detail for the base-case design. Much more work needs to be done, but at this point it appears that the design is feasible and will approach the design goal of supporting two commercial power reactors with each target/blanket module.

REFERENCES

1. Falter, H. D. et al., “Tests of High-Heat-Flux Target Plates for the JET Divertor,” American Nuclear Society Transactions, November 1991, pp. 655-666.
2. Celata, G. P. et al., “Burnout in Highly Subcooled Water-Flow Boiling in Small-Diameter Tubes,” American Nuclear Society Transactions, November 1991, pp. 657-658.
3. 130yd, R. D., "Subcooled Flow Boiling Critical Heat Flux (CHF) and its Application to Fusion Energy Components,” Fusion Technology, Vol. 7, January 1985, pp. 7-30.

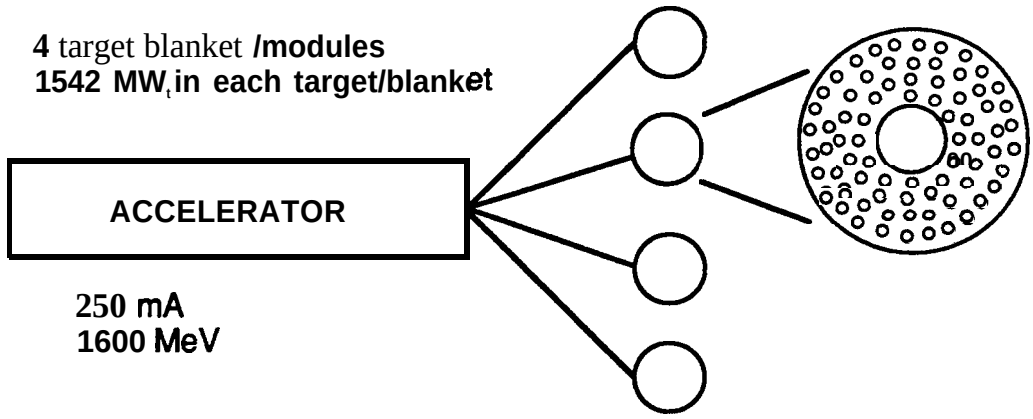

Fig. 1.
A'IW schematic.

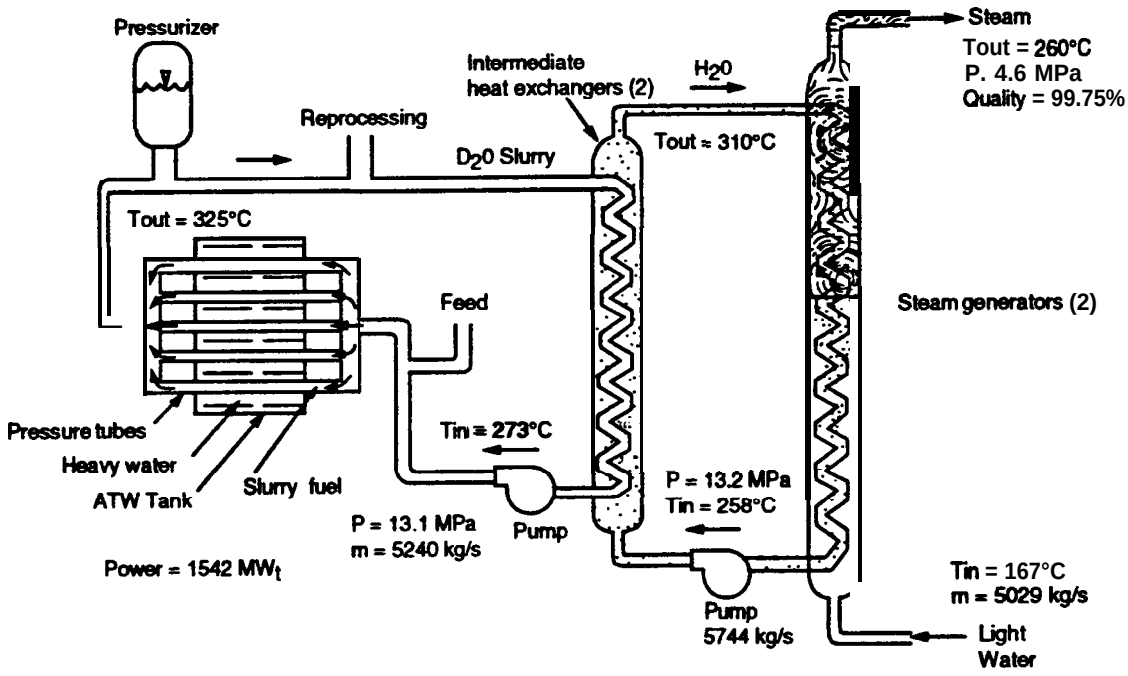

Fig. 2.
ATW balance of plant for the actinide slurry.

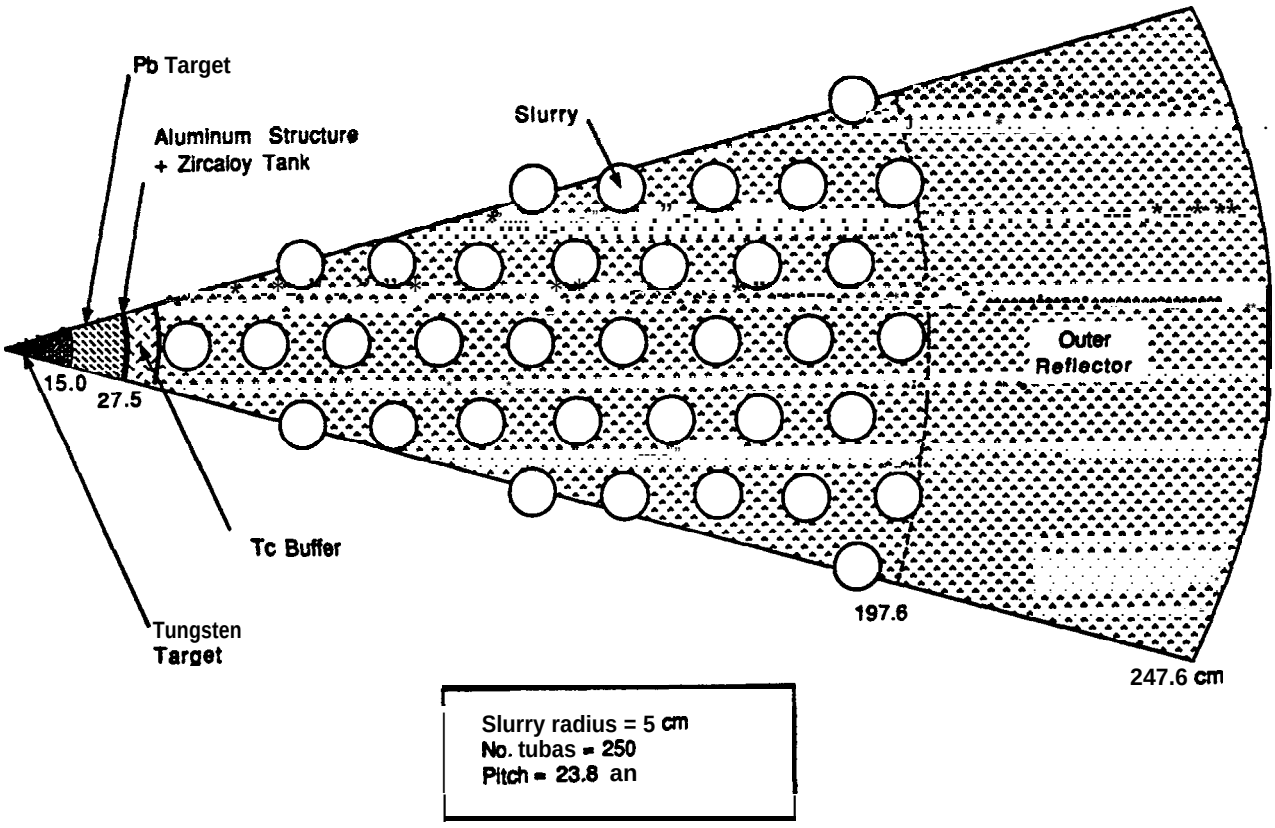

Fig. 3.
ATW target/blanket layout.

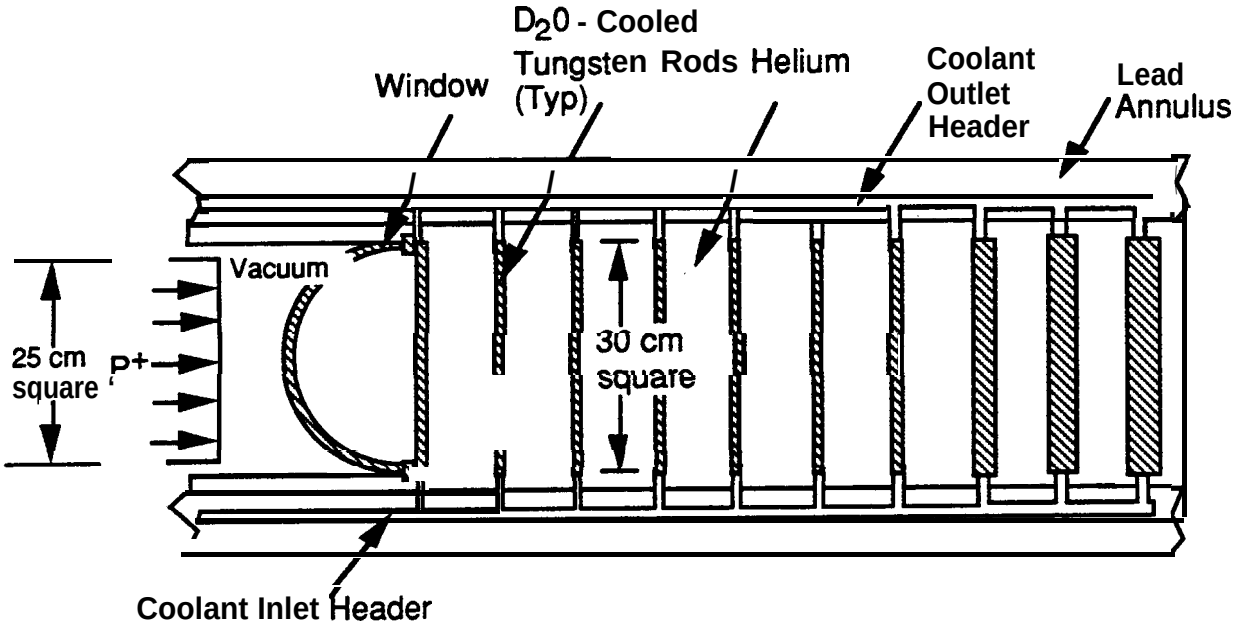

Fig. **4.**
Solid target design.

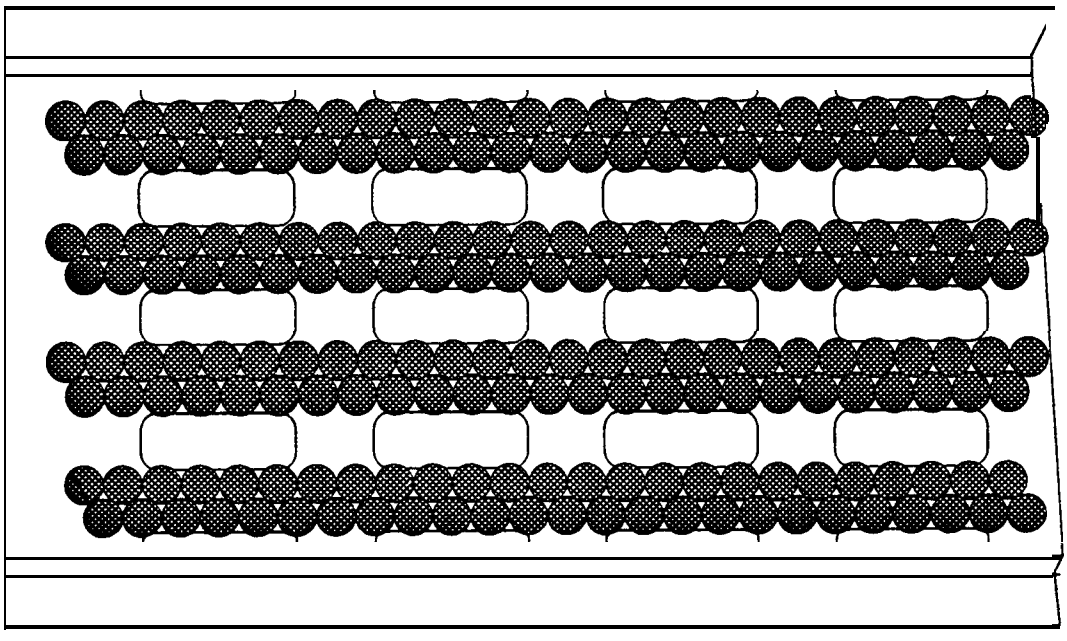

Fig. **5.**
End view of the tungsten rod unit.

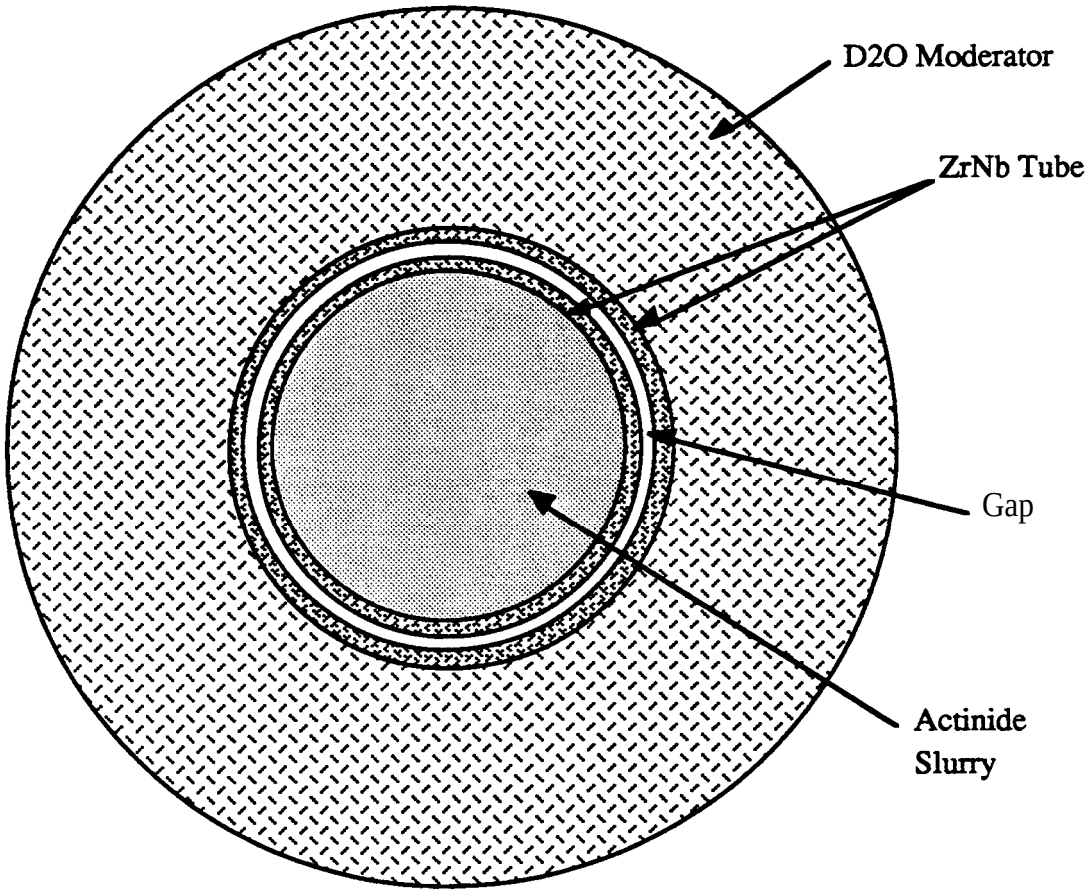

Region	Radius (cm)	Thickness (cm)	Volume Fraction
slurry	5.0		0.160
Inner Tube	5.42	0.42	0.028
Gap	5.81	0.39	0.028
Outer Tube	6.23	0.42	0.032
Moderator	12.52	6.29	0.752

Pitch = 23.8 cm (9.4 in.)

Fig. 6.
Blanket lattice cell.

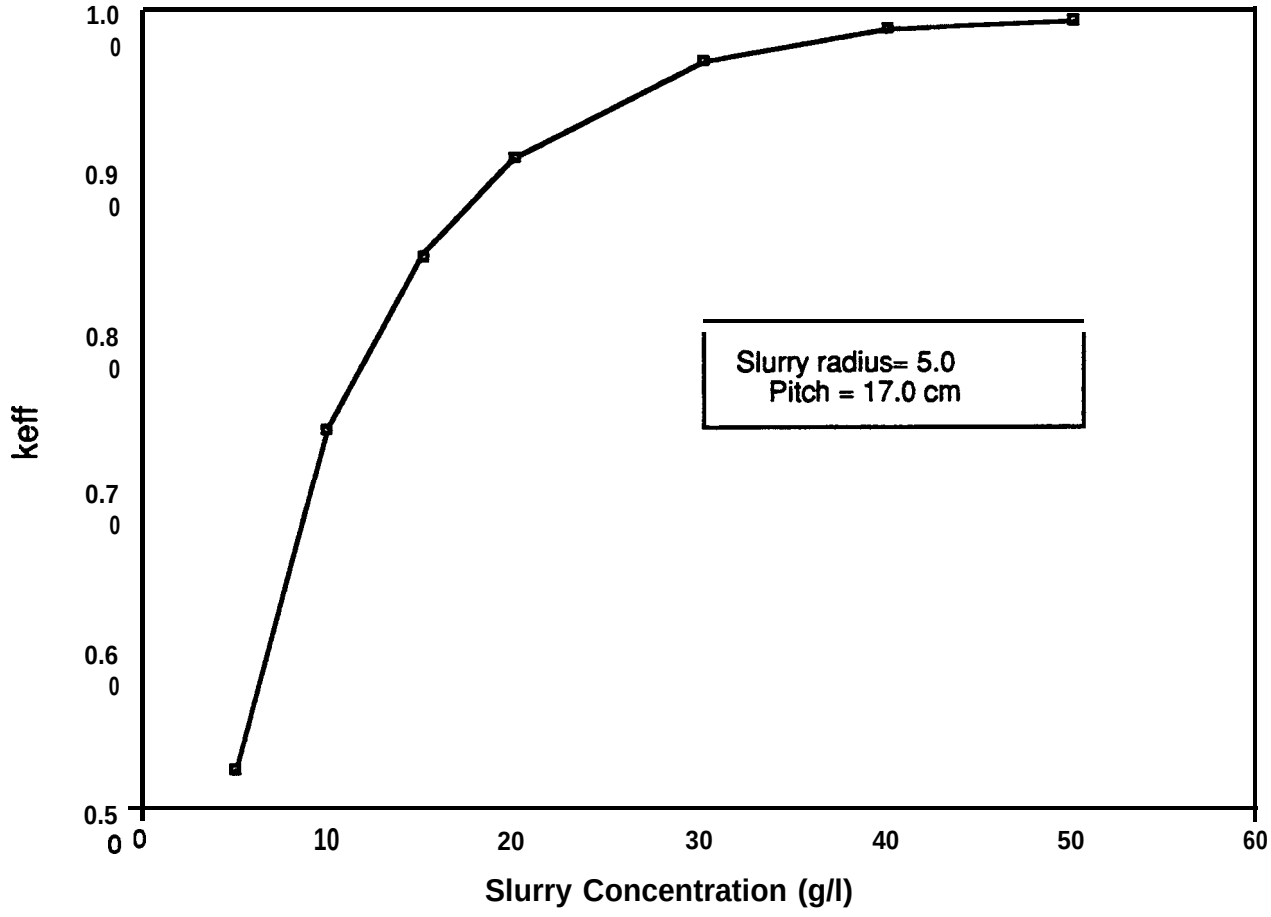

Fig. 7.
k_{eff} vs slurry concentration for the cell calculation.

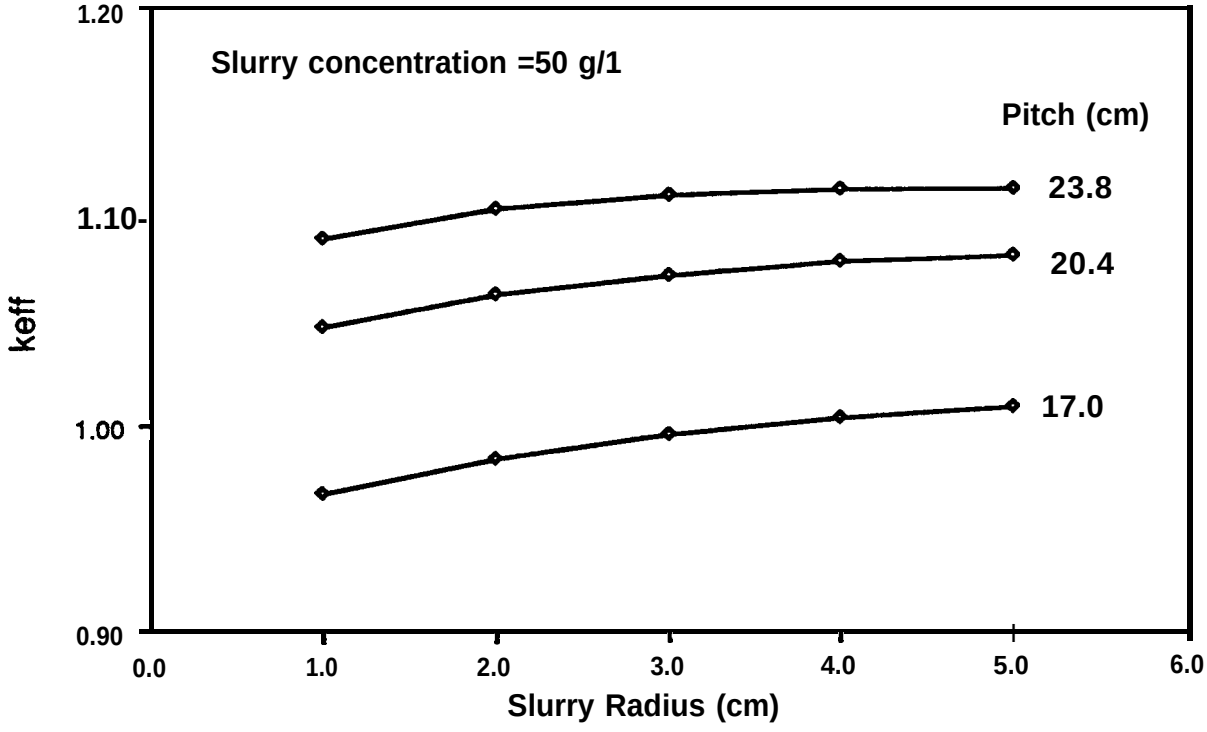

Fig. 8a.
k_{eff} vs shiny radius.

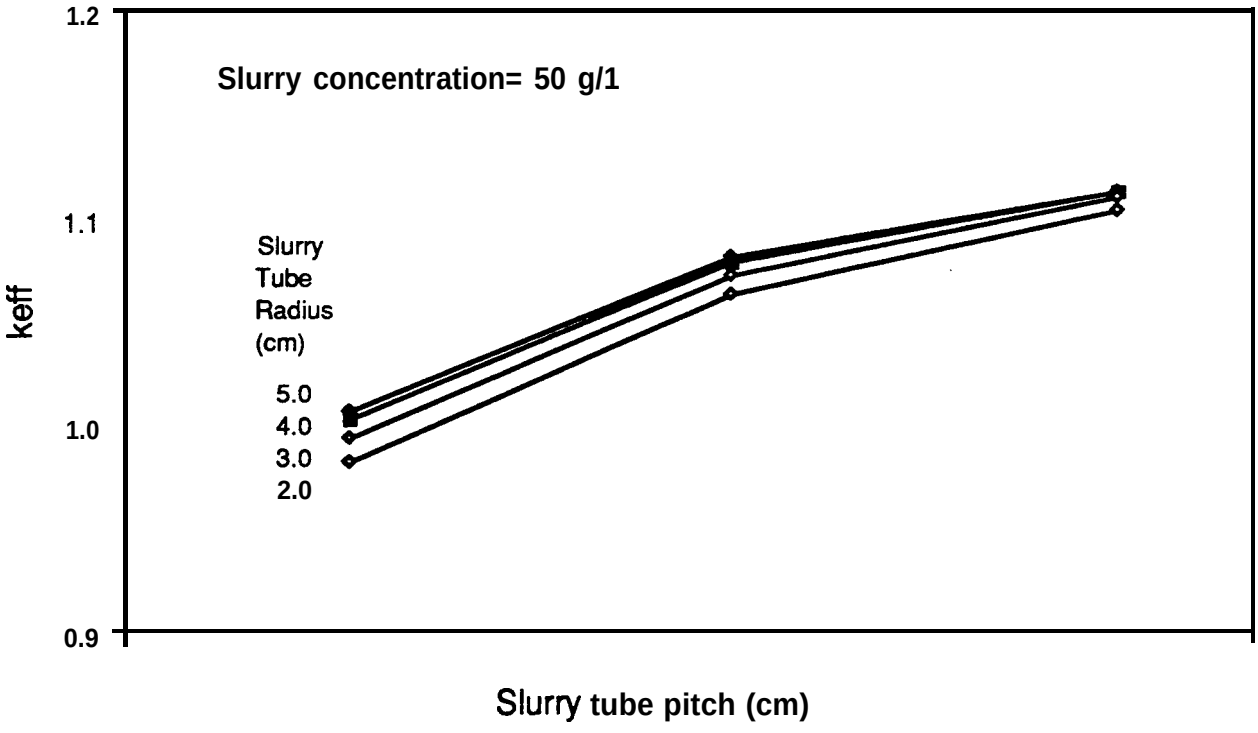

Fig. 8b.
k_{eff} vs slurry tube pitch.

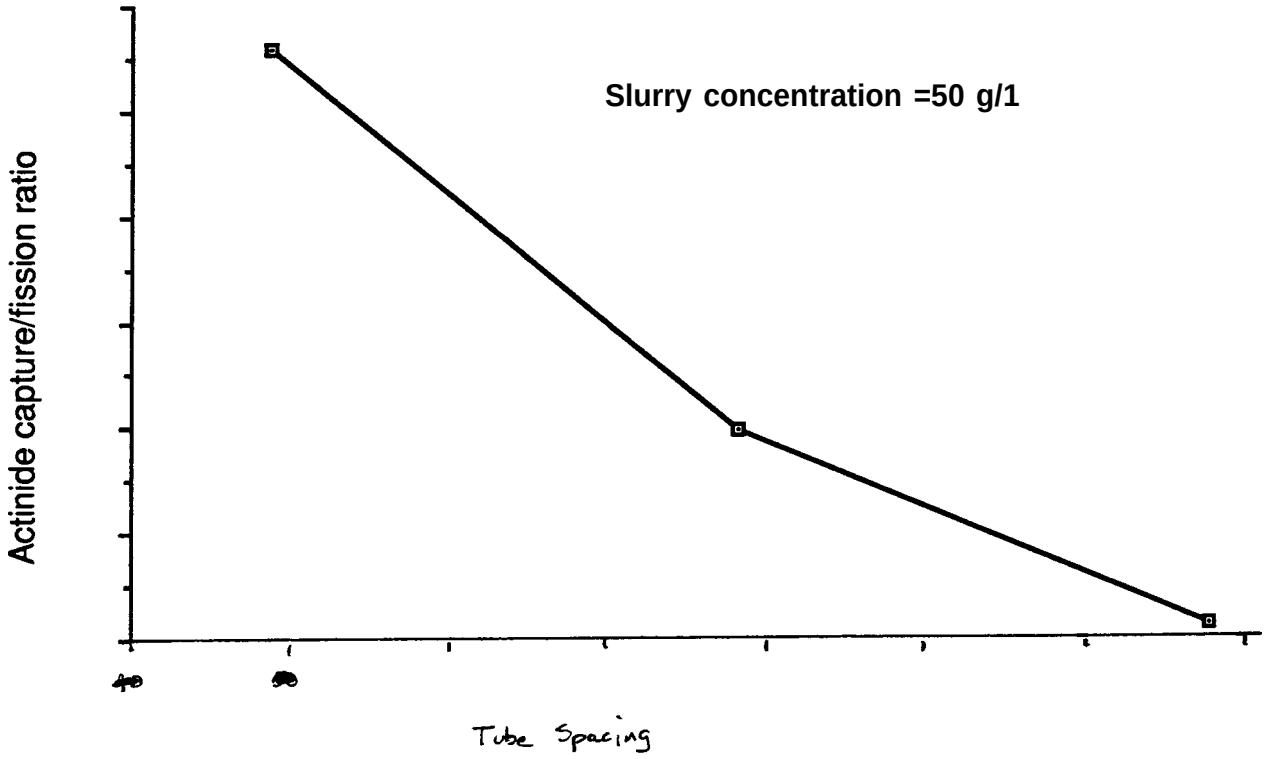

Fig. 9.
Capture/fission ratio vs slurry tube spacing.

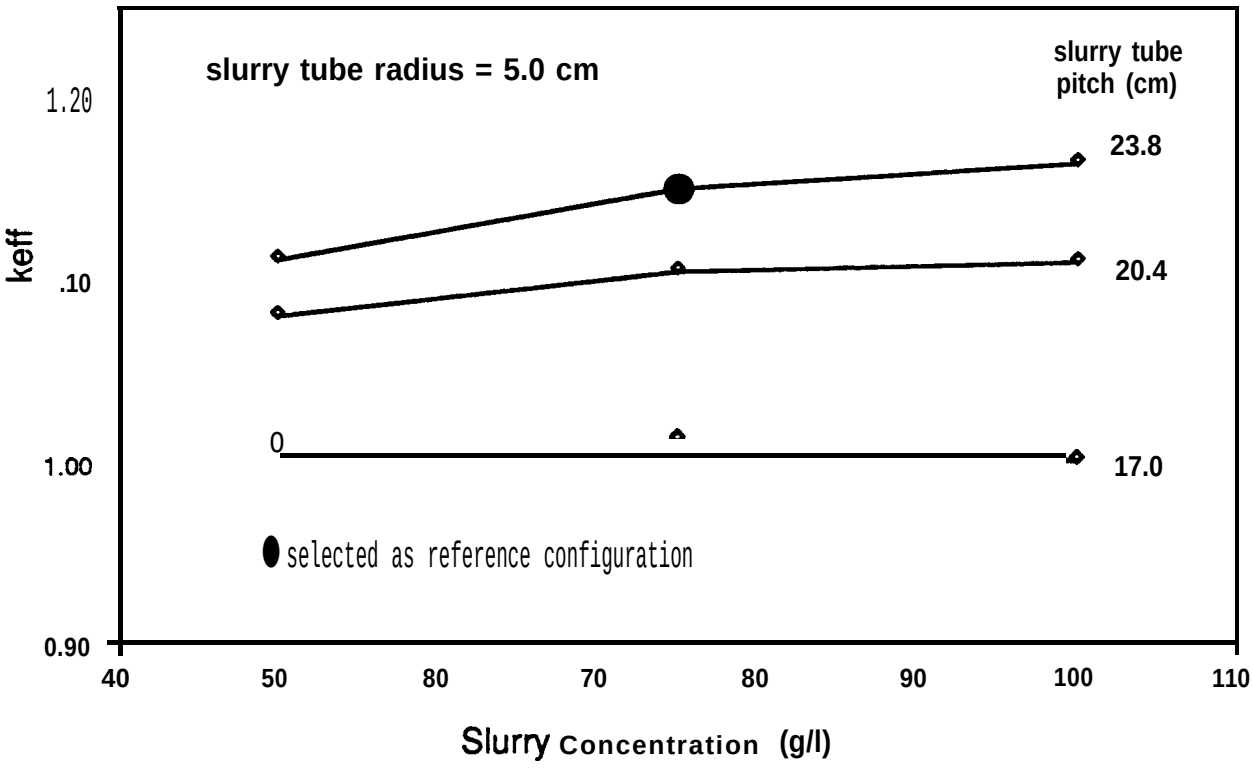

Fig. 10.
k_{eff} vs slurry concentration.

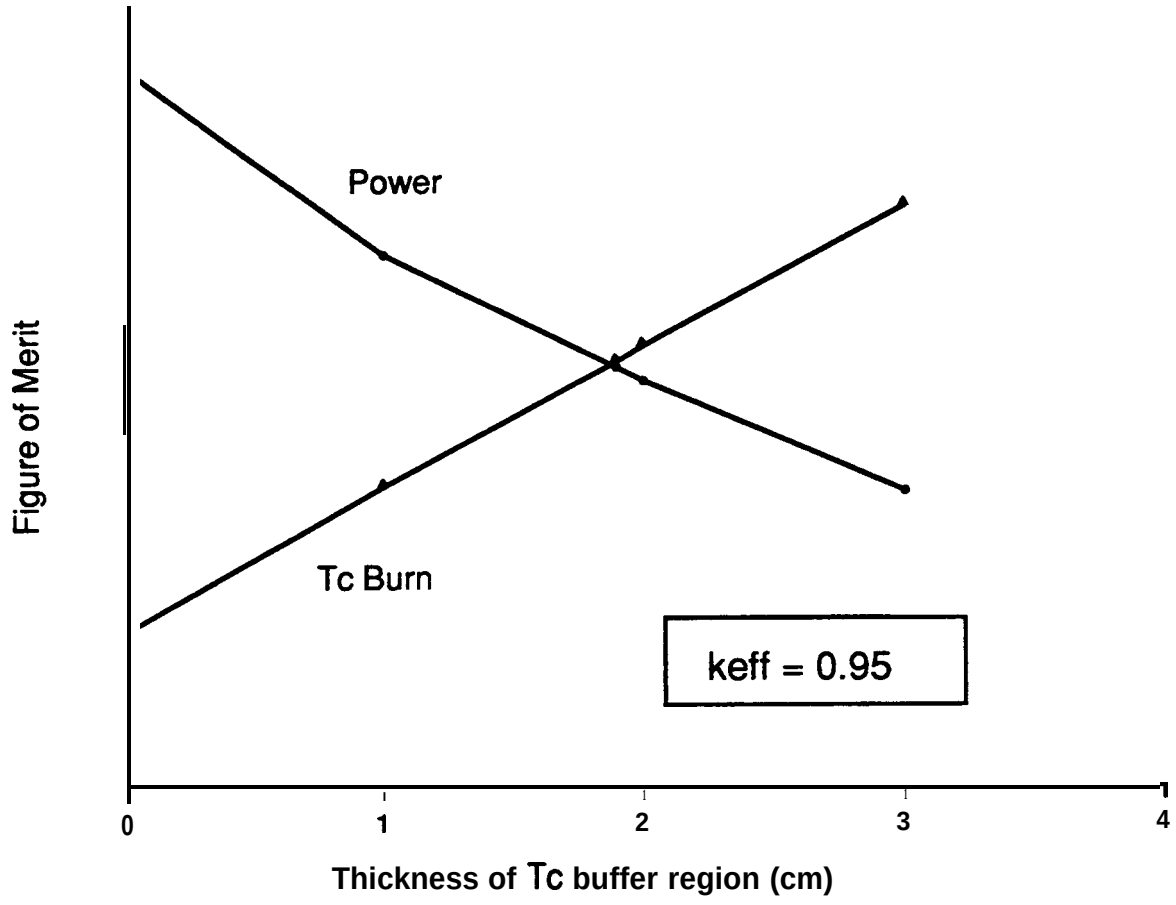

Fig. 11.
Blanket performance at k_{eff} of 0.95.

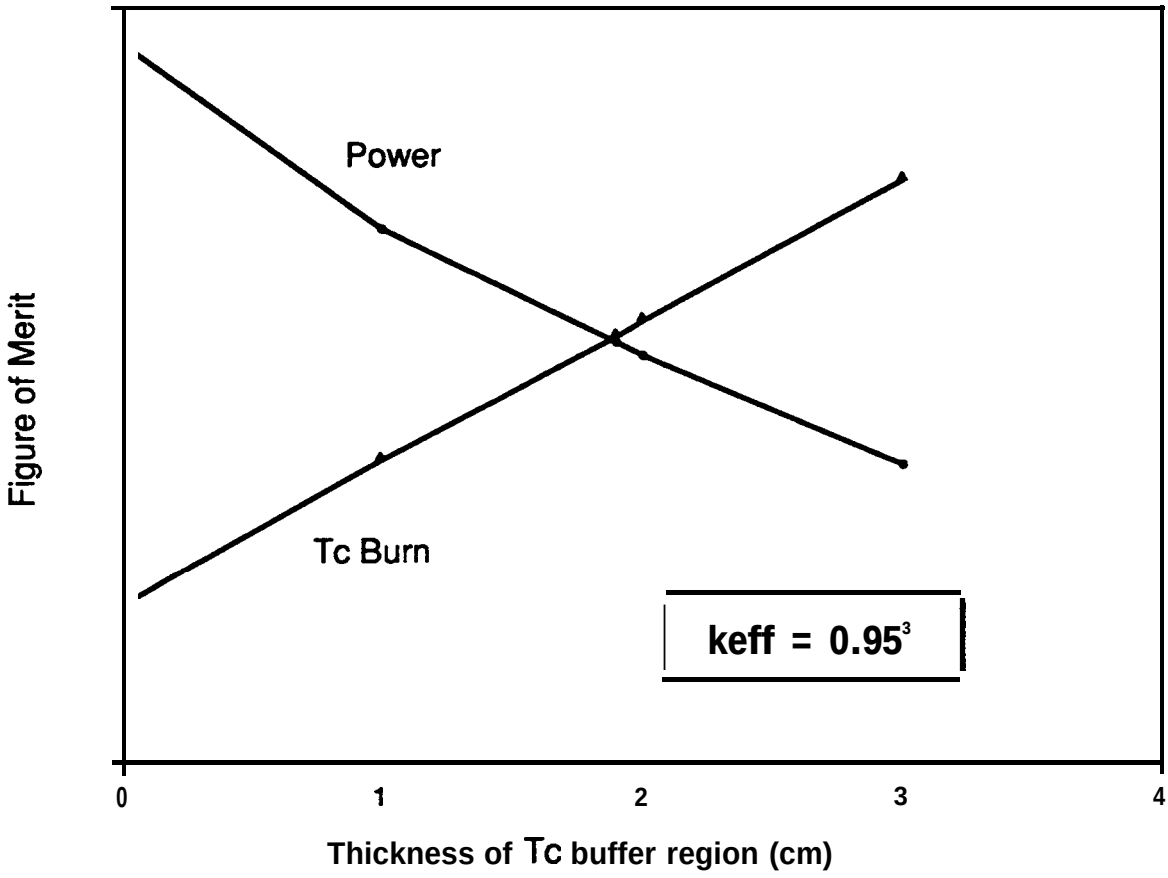

Fig. 12.
Blanket performance at k_{eff} of 0.93.

TABLE 1
KEY DESIGN PARAMETER COMPARISON

PARAMETER	CANDU-3	ATW
1. Blanket Arrangement		
Type	horizontal pressure tube	same
coolant	pressurized heavy water	same
Moderator	heavy water	same
Number of Fuel Assemblies	232	250
Fuel Assembly Material	Zirconium-Niobium	same
Total mass of Fuel	53174 kg	1550 kg
		(total primary loop)
k_{eff}	1.0	0.95
2. Fuel		
Fuel	compacted/sintered	aqueous actinide
	natural UO_2 pellets	solution (75 gin/l);
		(Pu, Np, Am, Cm)
Form	fuel bundle assembly;	flowing fuel solution
	37 elements/assembly	
Bundle Length	0.495 m	
Bundle Outer Diameter	0.1024 m	0.10 m
Bundles/Fuel Assembly	12	
3. **Heat Transport System**		
Number of Steam Generators	2	same
Steam Generator Type	vertical u-tube	same
Number of Heat-Transport Pumps	2	same
Pump Type	vertical, centrifugal, single	same
	suction, double discharge	
Number of Intermediate Heat Exchangers (II-IX)		2
IHX Type		vertical once-through
Number of IHX Pumps	-	2

PARAMETER	CANDU-3	ATW
IHX Pump Type		vertical, centrifugal
		single suction, double
		discharge
Blanket Outlet Pressure	9.9 MPa	13.1 MPa
Blanket Outlet Temp.	310 c	325 C
Blanket Inlet Temp.	258 C	273 C
Total Flowrate	5300 kg/s	5240 kg/s
Steam Outlet Temp.	260 c	same
Feedwater Inlet Temp.	187 C	same
steam Quality	99.75%	same
Steam Pressure	4.6 MPa	same
IHX outlet Temp.		310 c
IHX Outlet Pressure		13.2 MPa
IHX Inlet Temp.		258 C
IHX Flowrate		5744 kg/s
4. Power		
Total Fission Heat	1440.3 MW_t	1542 MW_t
Net Electrical Output	450 MWe	487 MWe

TABLE 2

RELATIVE ISOTOPIC COMPOSITIONS

Isotope	PWR Discharge	Equilibrium PHI=1.0E15
^{237}Np	0.0449	0.0317
^{238}Np	0.0000	0.0003
^{239}Np	0.0000	0.0000
Total Np	0.0449	0.0321
^{238}Pu	0.0140	0.0230
^{239}Pu	0.5148	0.0610
^{240}Pu	0.2372	0.1003
^{241}Pu	0.0785	0.0467
^{242}Pu	0.0481	0.2630
^{243}Pu*	0.0000	0.0002
^{244}Pu*	0.0000	0.0026
Total Pu	0.8925	0.4968
^{241}Am	0.0513	0.0048
^{242}Am	0.0000	0.0001
^{242m}Am*	0.0001	0.0001
^{243}Am	0.0092	0.0874
^{244}Am*	0.0000	0.0000
^{244m}Am*	0.0000	0.0000
^{245}Am*	0.0000	0.0000
Total Am	0.0607	0.0924
242Cm	0.0000	0.0213
243 Cm*	0.0000	0.0006
244Cm	0.0018	0.2794
245 Cm'	0.0001	0.0051
246 Cm*	0.0000	0.0004
247 Cm*	0.0000	0.0094
248 Cm*	0.0000	0.0625
240 Cm*	0.0000	0.0000
Total Cm	0.0019	0.3787
	1.0000	1.0000

•Multigroup cross sections not currently available.

TABLE 3

LATTICE CELL NEUTRON BALANCE

Isotope	Absorption	Fissions
^{237}Np	0.0219	0.0000
^{238}Np	0.0026	0.0024
^{239}Np	0.0000	0.0000
^{238}Pu	0.0435	0.0014
^{239}Pu	0.2777	0.1928
^{240}Pu	0.1513	0.0002
^{241}Pu	0.2594	0.1915
^{242}Pu	0.0380	0.0003
^{241}Am	0.0122	0.0001
^{242}Am	0.0064	0.0053
^{243}Am	0.0439	0.0001
^{242}Cm	0.0020	0.0002
^{244}Cm	0.0243	0.0013
zirconium	0.1033	
D_2O	0.0134	
TOTAL	1.0000	0.3956

TABLE 4

REFERENCE BLANKET NEUTRON BALANCE

keff		0.95
Sources		
Accelerator		1.000
Fissions Neutrons		8.994
Total Sources		9.994
Absorption		
Tungsten Region		0.4146
Lead Region		0.0880
Al + Zirc		0.0330
Tc Buffer		0.1855
Zirc		0.0106
Active Blanket		
Slurry	7.338	
Clad	0.829	
Moderator	0.097	
Tc (Self + LWR)	0.427	
Total Active Banket		8.691
Outer Reflector		
Tc	0.044	
D_2O	0.020	
Total Outer Refl.		0.064
Total Abs.		9.487
Leakage		
Radial		0.167
Axial		0.343
Total Leakage		0.510
Total Losses		9.997
Fissions		3.072
Tc Captures		0.656